

## Pattern formation driven by an acid-base neutralization reaction in aqueous media in a gravitational field

A. Zalts,<sup>1</sup> C. El Hasi,<sup>1</sup> D. Rubio,<sup>1</sup> A. Ureña,<sup>2</sup> and A. D'Onofrio<sup>3,\*</sup>

<sup>1</sup>*Instituto de Ciencias, Universidad Nacional General Sarmiento, J. M. Gutiérrez 1150, B1613GSX, Los Polvorines, Provincia de Buenos Aires, Argentina*

<sup>2</sup>*Laboratorio de Sólidos Amorfos, Facultad de Ingeniería, Universidad de Buenos Aires, Paseo Colón 850, Buenos Aires, Argentina*

<sup>3</sup>*Grupo de Medios Porosos, Facultad de Ingeniería, Universidad de Buenos Aires, Paseo Colón 850, Buenos Aires, Argentina*

(Received 8 May 2007; revised manuscript received 25 October 2007; published 23 January 2008)

We report the hydrodynamic instabilities found in a simple exothermic neutralization reaction. Although the heavier aqueous NaOH solution was put below the lighter layer of aqueous HCl solution, fingering at the interface in a Hele-Shaw cell was observed. The reaction front, which propagates downward, becomes buoyantly unstable in the gravity field. The mixing zone length and wave number depend on the reactant concentrations. The mixing zone length increases and the wave number decreases when the reactant concentrations decrease.

DOI: 10.1103/PhysRevE.77.015304

PACS number(s): 47.20.-k, 82.40.Ck, 47.56.+r

The instability of reaction-diffusion fronts has received great attention during recent years. Most of these studies are focused on traveling chemical fronts, produced by autocatalytic reactions, where steep gradients of the hydrodynamically relevant properties such as density, surface tension, or viscosity produce fingering patterns. Chemical autocatalysis was used to study the effects of a chemical reaction triggering hydrodynamic Rayleigh-Taylor instabilities [1–3]. These instabilities occur when a denser fluid lies on top of a lighter one in the gravitational field [4,5]. The initially flat chemical front, which results from the coupling between the chemical reaction rate and the molecular diffusion [5,6], loses its stability due to buoyancy effects, developing a fingering pattern [7]. On the other hand, heat production due to the exothermic reaction and temperature rise are very important, because they may stabilize the exothermic descending front [8,9]. This effect can be controlled by applying external cooling along the sidewalls of the reactor [10]. Several numerical and experimental studies of the hydrodynamic instability of chemical systems [9–12] and the effect of the thermal diffusion on autocatalytic systems [13] have been reported. In these cases, the critical wave number depends not only on the difference of density between products and reactants but also on the velocity, thickness of the chemical front, and reactant concentrations [14]. Hydrodynamic instabilities in an acid-base reaction at the interface of an organic liquid (isobutyl alcohol or cyclohexane) and a basic aqueous solution were reported by Eckert and Grahn [11] and Eckert *et al.* [12]. In these systems, the dynamics are driven by internal sources of energy provided by the chemical reaction: the release of the enthalpy of proton neutralization provides solute and thermal gradients.

In this Rapid Communication we present, to the best of our knowledge, the first report of hydrodynamic instabilities produced by a neutralization reaction between aqueous solutions of a strong acid (HCl) and a strong base (NaOH), without introducing organic solvents or weak acids or bases. The experiments were performed in a two-layer system, placed in

two Hele-Shaw (HS) cells. Each HS cell was constructed with two Plexiglas plates ( $20 \times 20 \times 1.2 \text{ cm}^3$ ), separated by a U-shaped polymeric (high-density polyethylene) spacer that closes the cell at the bottom and sides for the lower cell and the top and sides for the upper, with a gap width of  $d=1.0 \text{ mm}$  (Fig. 1). The HS cells can be fixed vertically or horizontally. The two-layer system is formed of a lower aqueous NaOH solution (concentration  $C_b=0.100M$ ,  $0.030M$ , or  $0.010M$ ) containing bromocresol green as an acid-base indicator ( $0.0032M$  in all cases), and an upper region, with an acidic (HCl) solution of the same molar concentration ( $C_a$ ) as the base below. Cell filling was done by means of syringes. The lower cell was filled by injecting the basic solution plus pH indicator from the bottom. To fill the upper cell, the acid solution was poured in a container and aspirated from the top inlet with a syringe. When both cells were full, the container was removed and the cells were carefully put in contact to start the reaction.

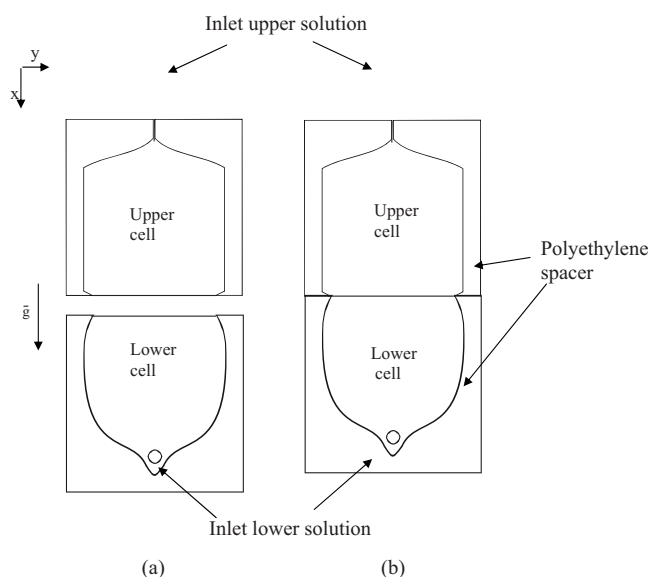


FIG. 1. Hele Shaw cells: (a) The cells are separated to fill with the solutions; (b) the cells are put in contact to start the reaction.

\*adonofr@fi.uba.ar

TABLE I. Densities ( $\delta$ ) of aqueous solutions.

Concentration (HCl, NaOH)	$\delta(\text{HCl})$ ( $\text{g}/\text{cm}^3$ )	$\delta(\text{NaOH} + \text{pH indicator})$ ( $\text{g}/\text{cm}^3$ )	Temperature ( $^{\circ}\text{C}$ )	$\Delta\delta$ between layers ( $\text{g}/\text{cm}^3$ )
0.010M	0.9977	0.9985	21.5	0.0008
0.030M	0.9980	0.9998	23.0	0.0018
0.100M	0.9987	1.0028	25.1	0.0041

The densities of the basic solutions plus pH indicator were always higher than those of the acidic solutions (Table I). Densities were measured with a precision of  $\pm 0.0001 \text{ g}/\text{cm}^3$  using an Anton Paar DMA 35N densimeter. Bromocresol green (BG) ( $pK_{a_{\text{BG}}} = 5.3$ ) was the chosen acid-base indicator because of its relatively high solubility and sharp color differences between acidic (bright yellow) and basic (dark blue) forms. We were able to follow experimentally the reaction front and the pattern formation through observing the color changes of the indicator. The HS cell was illuminated with transmitted diffuse white light and photographs were recorded at desired time intervals with a digital camera ( $3072 \times 2304$  pixels). Images were stored and processed with programs based on language C, developed in the laboratory, in order to obtain the interface position, the traveling front speed, the pattern wavelength, and the length of the mixing zone as a function of time. To determine the mixing zone, the program finds the front shape of every image. Then it calculates the region along the  $x$  axis (Fig. 1) where the average acid concentration lies between 5% and 95%. The length of this zone is considered the “length of the mixing zone.”

While in water NaOH is a strong base and HCl a strong acid, the reaction taking place is proton neutralization (reaction enthalpy  $\Delta H \sim -57 \text{ kJ}/\text{mol}$ ) to form  $\text{H}_2\text{O}$ . This is one of the fastest solution reactions:  $q$  for the forward reaction is  $1.4 \times 10^{11} \text{ l mol}^{-1} \text{ s}^{-1}$  and  $2.5 \times 10^{-5} \text{ l mol}^{-1} \text{ s}^{-1}$  for the reverse reaction [15]. The mobility of protons in water is about three times that of typical ions (Grotthus mechanism) due to a cooperative rearrangement of the atoms through a network of several hydrogen-bonded  $\text{H}_2\text{O}$  molecules. In their reaction with  $\text{OH}^-$ , ions whose mobility is also high, an equivalent quantity of water (the solvent) is formed. As the hydrated  $\text{Na}^+(\text{aq})$  and  $\text{Cl}^-(\text{aq})$  ions will diffuse from one layer into the other (without reacting, as the driving force is water formation), in the mixing zone these ions are the prevailing species. The densities of the initial acidic and basic solutions were measured (Table I), but we lack an experimental value for the density of the saline solution. The volume in the HS cell where the NaCl solution is formed is not known and we cannot take a representative sample of this solution without perturbing the whole system.

When both HS cells are put in contact in a vertical position, a horizontal front that propagates downward is formed [Figs. 2(a)–2(c)]. Depending on the reactant concentration, a characteristic structure with segments curved convexly toward the acidic phase develops at different times (fingers). To be sure that gravity  $g$  is important in the pattern formation, experiments with the HS in the horizontal position were performed [Fig. 2(d)]: as no pattern was observed in the

reaction front using the cells in this position, the released potential energy emerges from buoyancy. In all experiments, in either the vertical or horizontal position, the reaction front moves toward the basic solution because the acid has a higher diffusion coefficient than the base.

From Figs. 2(a) and 2(d) it is possible to verify that the rate of advance of the reaction front is consistent with a diffusive process with  $D \sim 10^{-5} \text{ cm}^2/\text{s}$ , of the same order as the diffusion coefficients of the involved species.

The pattern wavelength and length of the mixing zone also depend on reactant concentrations. Figure 3 shows the length of the mixing zone evolution as a function of time for different concentrations (0.010M, 0.030M, and 0.100M). In the case of using 0.010M solutions, a pattern is distinguishable after about 30 min of contact and further evolution of the pattern and the length of the mixing zone is observed at any time. For 0.030M solutions, although the mixing zone length increases as a function of time, it is always smaller than that observed with 0.010M solutions for the same time. For 0.100M solutions, once the instability is formed, no further evolution is observed during the next 7 days (Figs. 2 and 3).

Power spectral densities for different concentrations are shown in Fig. 4. For reactant concentrations of 0.010M, 0.030M, and 0.100M, the wave numbers  $k$  are 1.16, 2.80, and  $3.80 \text{ mm}^{-1}$ , respectively. The power spectral density  $P$  of the wave number  $k$  with maximum growth rate  $\sigma_k$

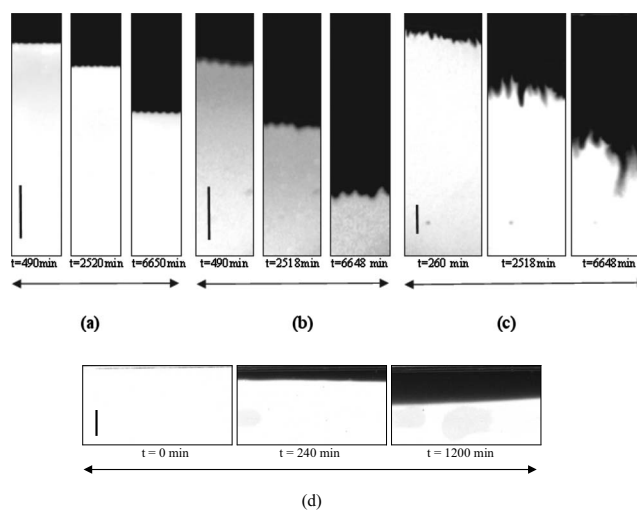


FIG. 2. Experimental image, for (a) 0.100M, (b) 0.030M, and (c) 0.010M solutions at different times (vertical position). (d) 0.010M solution at different times (horizontal position). Light zones correspond to basic phase and dark zones to acidic phase. Scale: Vertical black bar = 1 cm.

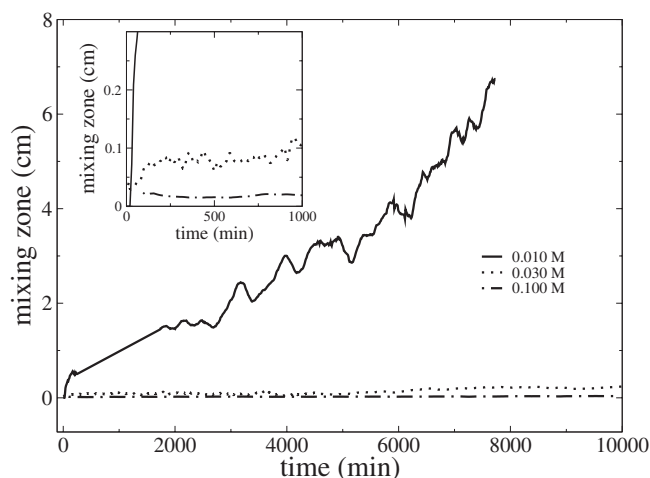


FIG. 3. Variations of the mixing zone (lower half Hele-Shaw cell) as a function of time for different reactant concentrations.

( $k=3.80 \text{ mm}^{-1}$ ) as a function of time, for  $0.100M$  solutions, is shown in Fig. 5. We can see that at early times (2000 min) there is a growing amplitude ( $\sigma_k \neq 0$ ); for longer times, the amplitude remains constant ( $\sigma_k \approx 0$ ). Wave numbers were obtained from the images (some of them are shown in Fig. 2) by applying a one-dimensional Fourier transformation to the interface.

The wave number with maximum growth rate increases with solution concentration. The same behavior was found in experimental and numerical works with the chlorite-tetrathionate (CT) reaction [2,16], where an increase in the concentration is observed to produce an increase in the wave number. A further increase in concentration can lead to a pattern with such a high wave number that a flat front is obtained. Figure 4 also shows that the amplitude (proportional to the wave number power) for the  $0.010M$  solutions is more than ten times higher than that obtained for  $0.030M$  and  $0.100M$  solutions. This is in agreement with the finger amplitudes observed in Fig. 2.

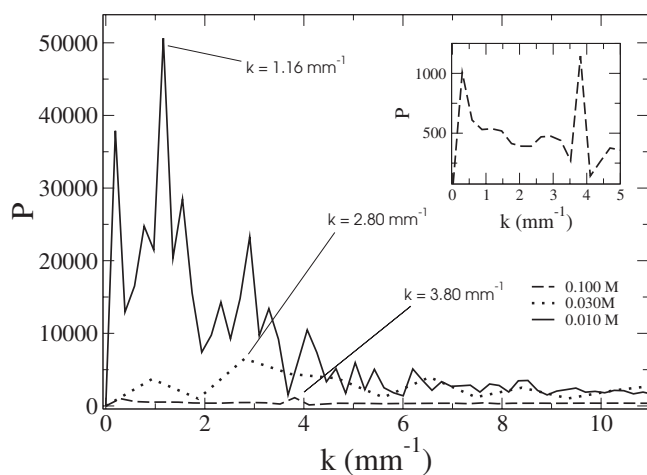


FIG. 4. Power spectral densities  $P$  of the fingers for different concentrations ( $t=6648 \text{ min}$ ). Note that the basic modes increase when the solution concentration increases.

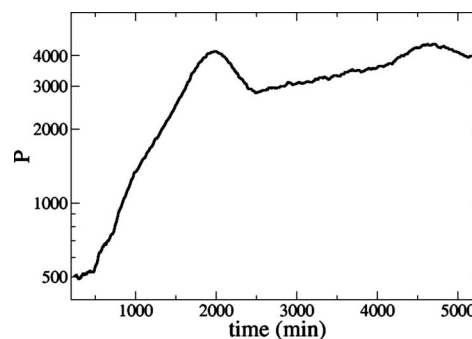


FIG. 5. Power spectral density  $P$  of the wave number with maximum growing rate ( $k=3.8 \text{ mm}^{-1}$ ) as a function of time, for  $0.100M$  solutions, obtained from Fourier transformation.  $P$  stabilizes for  $t > 2000 \text{ min}$ .

Although the origin of this instability is not known, possible driving forces might be related to phenomena such as local density increase due to salt production, local density decrease by temperature rise and dilution due to water formation, or a large difference between the diffusion coefficients of the reacting species.

Density changes at the interface could be expected when a heavier product (e.g., NaCl) than the reactant (NaOH) is obtained in the mixing zone [17]. On the other hand, as the neutralization reaction is exothermic, heat release could produce a local density decrease in the HCl solution at the reaction front. As this hotter solution lies below the rest of the HCl solution, still at room temperature, the system becomes unstable.

We observed that a chemical reaction can trigger a buoyancy-driven instability across the interface separating two hydrodynamically stable fluids. In this case, although a fluid of lesser density was placed on top of a denser one, once the reaction takes place, the system leads to instabilities due to gravity field effects. The results depend strongly on the reactant concentrations. The mixing zone increases as the reactant concentration decreases. As an increase of reactant concentration produces an increase in the wave numbers, flat fronts could be expected with still higher reactant concentrations than those used in this work.

Although in this study, as well as in previous work by Eckert and co-workers [11,12], instabilities are observed when a hydrodynamically stable system is coupled with an acid-base neutralization reaction, our system is based exclusively on aqueous solutions of a strong acid and base. This experimental modification rules out several experimental constraints that are present in a two-layer case that uses an immiscible organic solvent containing the acidic species and water as solvent for the basic species. In our case, as water is the solvent in both layers, we avoid effects due to surface tension; the layers have almost the same viscosity, so viscous fingering can be ruled out; there is no need to consider partial solubilities between an organic solvent and water and their effect on the acid partition between the two layers. Using only aqueous solutions, the neutralization will be limited by diffusion of the reactive species and there is no need to consider the rate at which the acidic species crosses the immiscible solvent boundary. As a consequence, we worked with

time scales on the order of hours or days to observe different patterns in moving fronts instead of time scales of seconds and a mixing zone that broadens near the interface. In our system, employing only aqueous layers, a completely different fingering pattern is produced because the behavior of the species is different.

Pojman *et al.* [18] observed convection and fingering when an aqueous solution of sulfuric acid was put in contact with a sodium sulfate solution, whose concentrations were selected to put the less dense solution always on top before the experiment was triggered. In this case, the larger diffusion coefficient of sulfuric acid ( $2.9 \times 10^{-5} \text{ cm}^2/\text{s}$ ) was the cause of the instability: one species must have a diffusion coefficient at least three times larger than the other species. For a descending front, Pojman *et al.* describe a weak convection due to this diffusion coefficient difference that produces fingering observable on time scales of a few minutes. In our case, HCl has the larger diffusion coefficient ( $1.41 \times 10^{-5} \text{ cm}^2/\text{s}$ ), but compared with NaOH ( $1.07 \times 10^{-5} \text{ cm}^2/\text{s}$ ), the ratio is 1.3. We observed that the acid enters into the basic solution and a moving front toward the basic layer is obtained, whenever the cell is in the vertical or horizontal position. As the fingering regime is produced in the vertical position, and a flat front is observed in the horizontal position for the same chemical composition, the fingering phenomenon is gravity related. As both reactants move fast and a dilution in the mixing zone is produced due to water formation when neutralization takes place, a concentration depletion of the acid on top of the interface can be expected, leading to a Rayleigh-Taylor instability. So, after the onset of the instability, the movement of the species will no longer be diffusive but convective. At higher concentrations, the difference in densities between the layers is higher (Table I), slowing down the fingering process. At higher reactant concentrations, the neutralization reaction proceeds faster, segregating the reactants soon after the cells are put in contact. Once the segregation is established, the density difference between the reactants stabilizes the dynamics and the instability is “frozen” at the acid-salt interface and no convective movement is observed. In fact, using 0.1M solutions,

the reaction front moves at a rate consistent with a diffusive process, without disturbing the wave pattern. At lower concentrations the convective movement can proceed without the initial density stabilizing effect, leading to a fingering process.

On the other hand, there are many studies reported on instabilities observed in autocatalytic reactions. Results obtained with this kind of reaction (by Lima *et al.* [2] and Bánsági *et al.* [16], changing reactant concentrations in chlorite-tetrathionate (CT) experiments, or Epstein and Pojman [7], for example), show that the chemical reaction favors planar fronts, leading to a more effective coarsening in the nonlinear fingering regime. For CT experiments, as well as in the acid-base system presented here, moving fronts are observed. In CT experiments the reactants are mixed throughout the cell before the reaction takes place, leading to a constant reaction rate and a genuinely unstable Rayleigh-Taylor density stratification. In this case (CT experiment) the front movement is related to the chemical reaction rate. It remains as an open question which pathway is responsible for the observed instabilities in the acid-base neutralization.

As a conclusion, we report that an acid-base reaction between aqueous HCl and NaOH solutions can lead to instabilities due to gravitational field effects when the components in a hydrodynamically stable two-layer system, with a simpler chemical composition than those previously reported in the literature, are put in contact using vertical HS cells. The initial concentration of the reactants determines the dynamics of the reactive front, pattern formation, and interface growth rate. Clearly, there is a reactant concentration at which a transition from diffusive to convective movement takes place. Further studies are needed to fully understand this system. In particular, numerical simulations will provide a better insight into the reactant and product concentrations, as well as the density profile through the mixing zone.

The authors thank Emilio Winograd and Leandro Lanosa for experimental support and A. De Wit and D. Strier for fruitful discussions. This work was supported by CONICET (Argentina), FNRS (Belgium), UBA, and UNGS.

- 
- [1] J. Yang, A. D’Onofrio, S. Kalliadasis, and A. De Wit, *J. Chem. Phys.* **117**, 9395 (2002).
- [2] D. Lima, A. D’Onofrio, and A. De Wit, *J. Chem. Phys.* **124**, 014509 (2006).
- [3] M. Böckmann and S. C. Müller, *Phys. Rev. E* **70**, 046302 (2004).
- [4] S. Chandrasekhar, *Hydrodynamic and Hydromagnetic Stability* (Clarendon, Oxford, 1961).
- [5] J. D. Murray, *Mathematical Biology* (Springer, Berlin, 1989).
- [6] S. K. Scott, *Chemical Chaos* (Oxford University Press, Oxford, 1991).
- [7] I. R. Epstein and J. A. Pojman, *An Introduction to Nonlinear Chemical Dynamics* (Oxford University Press, Oxford, 1988).
- [8] G. García Casado, L. Tofaletti, D. Müller, and A. D’Onofrio, *J. Chem. Phys.* **126**, 114502 (2007).
- [9] J. D. Hersoncourt, S. Kalliadasis, and A. Wit, *J. Chem. Phys.* **123**, 234503 (2005).
- [10] D. A. Bratsun, Y. Shi, K. Eckert, and A. De Wit, *Europhys. Lett.* **69**, 746 (2005).
- [11] K. Eckert and A. Grahn, *Phys. Rev. Lett.* **82**, 4436 (1999).
- [12] K. Eckert, M. Acker, and Y. Shi, *Phys. Fluids* **16**, 385 (2004).
- [13] B. F. Edwards, J. W. Wilder, and K. Showalter, *Phys. Rev. A* **43**, 749 (1991).
- [14] D. A. Vasquez, B. F. Edwards, and J. W. Wilder, *Phys. Fluids* **7**, 2513 (1995).
- [15] D. F. Shriver, P. W. Atkins, and C. H. Langford, *Inorganic Chemistry*, 2nd ed. (Oxford University Press, Oxford, 1998).
- [16] T. Bánsági, Jr., D. Horváth, and Á. Tóth, *Chem. Phys. Lett.* **384**, 153 (2004).
- [17] O. Citri, M. L. Kagan, R. Kosloff, and D. Avnir, *Langmuir* **6**, 560 (1990).
- [18] J. A. Pojman, A. Komlósi, and I. P. Nagy, *J. Phys. Chem.* **100**, 16209 (1996).